Thermophilic ATP synthase has a decamer *c*-ring: Indication of noninteger 10:3 H^+/ATP ratio and permissive elastic coupling

Noriyo Mitome*, Toshiharu Suzuki*†, Shigehiko Hayashi‡§, and Masasuke Yoshida*†¶

*Chemical Resources Laboratory, Tokyo Institute of Technology, Nagatsuta 4259, Yokohama 226-8503, Japan; †ATP System Project, Exploratory Research for Advanced Technology (ERATO), Japan Science and Technology Agency, Nagatsuta 5800-3, Yokohama 226-0026, Japan; ‡Fukui Institute for Fundamental Chemistry, Kyoto University, Kyoto 606-8103, Japan; and §Precursory Research for Embryonic Science and Technology (PRESTO), Japan Science and Technology Agency, 4-1-8 Honcho Kawaguchi, Saitama 332-0012, Japan

Edited by Paul D. Boyer, University of California, Los Angeles, CA, and approved June 14, 2004 (received for review May 20, 2004)

In a rotary motor F_oF_1-ATP synthase that couples H^+ transport with ATP synthesis/hydrolysis, it is thought that an F_oc subunit oligomer ring (*c*-ring) in the membrane rotates as protons pass through F_o and a 120° rotation produces one ATP at F_1. Despite several structural studies, the copy number of F_oc subunits in the *c*-ring has not been determined for any functional F_oF_1. Here, we have generated and isolated thermophilic *Bacillus* F_oF_1, each containing genetically fused 2-mer–14-mer *c* (c_2–c_{14}). Among them, F_oF_1 containing c_2, c_5, or c_{10} showed ATP-synthesis and other activities. When F_1 was removed, F_o containing c_{10} worked as an H^+ channel but F_os containing c_9, c_{11} or c_{12} did not. Thus, the *c*-ring of functional F_oF_1 of this organism is a decamer. The inevitable consequence of this finding is noninteger ratios of rotation step sizes of F_1/F_o (120°/36°) and of H^+/ATP (10:3). This step-mismatch necessitates elastic twisting of the rotor shaft (and/or the side stalk) during rotation and permissive coupling between unit rotations by H^+ transport at F_o and elementary events in catalysis at F_1.

The F_oF_1-ATP synthase, often simply called F_oF_1, is composed of two portions: a water-soluble F_1, which has catalytic sites for ATP synthesis and hydrolysis, and a membrane-integrated F_o, which mediates H^+ (proton) transport (1, 2). When isolated, F_1 has ATP-hydrolyzing activity and F_o acts as a proton channel. The bacterial F_oF_1 has the simplest subunit structure, $\alpha_3\beta_3\gamma\delta\varepsilon$ for F_1 and ab_2c_n for F_o (where *n* is the copy number of the *c* subunits), as depicted schematically in Fig. 1*A*. F_1 and F_o are motors that share a common central rotor; a down-hill proton flow through F_o drives rotation of the rotor, causing conformational changes in F_1 that result in ATP synthesis. Conversely, ATP hydrolysis in F_1 causes a reverse rotation of the rotor that enforces F_o to pump protons to the reverse direction. The ring of F_oc subunit oligomer and the γ-ε subunits of F_1 comprise the central rotor, and they rotate together as a single body (3). The side stalk made up of δ-b_2 subunits connects the membrane-bound F_oa subunit with the $\alpha_3\beta_3$ hexamer ring of F_1, which prevents the hexameric ring from rotating as γ subunit rotates. Rotary motion of F_1 has been analyzed in detail, and it has been established that the γ subunit rotates with a discrete 120° step per each consumed ATP (4, 5) (three ATP molecules per revolution). However, little is known about the F_o rotation. It has been proposed that each proton is first transported to a glutamic acid of an F_oc subunit of the *c*-ring, which is located at the middle of a transmembrane helix of F_oc, through a channel in the periplasmic half of the F_oa subunit, and then after one revolution of the *c*-ring, the proton is released to cytoplasm through another half-channel of F_oa (6, 7) (Fig. 1*A*). In this mechanism, the copy number of F_oc in the *c*-ring should be equal to the number of transported protons per revolution of the *c*-ring that directly defines the H^+/ATP ratio, which is one of the most important parameters in bioenergetics. Structural studies have suggested different copy numbers of F_oc in the ring, depending on the sources. There are 10 copies of F_oc in an yeast mitochondrial F_1–F_oc complex (crystal structure) (8), 11 copies in the *c*-oligomers isolated from *Ilyobacter tartaricus* (atomic-force microscopy and transmission cryoelectron microscopy) (9), and 14 copies of *c*-oligomers isolated from chloroplasts (atomic-force microscopy) (10, 11). A cross-linking study suggested 10 copies as a preferred number of F_oc in *Escherichia coli* F_oF_1 (12). However, no conclusive evidence of the copy number in the functional F_oF_1 complex has been obtained because the results cited above were obtained for the *c*-ring of subcomplex lacking all other F_o subunits (8), for the *c*-oligomers extracted with SDS or other detergents (9–11), or by an indirect method (12). In this study, we have generated functional F_oF_1–ATP synthase whose proton-translocating *c*-ring is made from a single-polypeptide chain of 10 tandemly fused *c* subunits and discussed in terms of elastic coupling between F_o and F_1.

Materials and Methods

F_oF_1s with Fused Multimer F_oc. An *Avr*II restriction site was introduced to the expression plasmid pTR19-ASDS (13) for thermophilic *Bacillus* PS3 F_oF_1 by the megaprimer method (14). Appropriate oligonucleotide primers were annealed upstream of *uncB* (F_oa) and a 3′-region of antisense strand of *uncE* (F_oc). To introduce *Spe*I and *Nhe*I sites, a second PCR was carried out with the product of the first PCR as a template in the presence of the oligonucleotide primer that annealed to the downstream of *uncE*. The amplified DNA fragment was digested with *Eco*RI and *Spe*I and ligated to the pTR19-ASDS, digested previously with both restriction enzymes, to produce pTR19-AC1N. A plasmid pTR19-AC1 was also generated by the megaprimer method. The amplified product was digested with *Eco*RI and *Spe*I and inserted into the plasmid pTR19-ASDS, which was previously digested with both restriction enzymes. To prepare a tandemly fused dimeric *uncE* (c_2) gene, pTR19-AC1N was digested with *Eco*RI and *Nhe*I, and the 1.3-kbp *Eco*RI–*Nhe*I fragment was ligated into an *Eco*RI–*Avr*II site of pTR19-AC1 (plasmid pTR19-AC2). To obtain a plasmid having a fused trimeric *uncE* (c_3) gene, the *Eco*RI–*Nhe*I fragment of pTR19-AC1N was introduced into the *Eco*RI–*Avr*II site of pTR19-AC2 (pTR19-AC3). By using this procedure, *uncE* genes were fused one by one. Consequently, plasmids expressing 13 kinds of F_oF_1s that have tandemly fused F_oc 2-mer, 3-mer, 4-mer, 5-mer, 6-mer, 7-mer, 8-mer, 9-mer, 10-mer, 11-mer, 12-mer, 13-mer, or 14-mer (c_2–c_{14}) were prepared. The multimer *uncE* genes of the mutants were verified by restriction mapping of the plasmids. A plasmid to express a mutant F_oF_1 with a substitution of F_ocGlu-56 by Gln (E56Q) at the N-terminal hairpin in c_{10} was constructed by the

This paper was submitted directly (Track II) to the PNAS office.

Abbreviations: DCCD, *N,N′*-dicyclohexylcarbodiimide; ACMA, 9-amino-6-chloro-2-methoxyacridine; FCCP, *p*-trifluoromethoxyphenylydrazone.

¶To whom correspondence should be addressed. E-mail: myoshida@res.titech.ac.jp.

method of Kunkel *et al.* (15). Plasmids for the wild-type and mutant F_oF_1s obtained, as described above, were individually expressed in an F_o-deficient *E. coli* strain JJ001 (*pyrE41*, *entA403*, *argHI*, *rspsL109*, *supE44*, Δ*uncBEFH*, *recA56*, *srl*::*Tn10*) (16) (a kind gift from J. Hermolin, University of Wisconsin Medical School, Madison). Culture of the transformants, preparation of membrane vesicles, solubilization and purification of F_oF_1, and reconstitution of the purified F_oF_1 into liposomes were performed as described (13). The F_oF_1s used in this work has a tag of 10 His residues at the N terminus of the β subunit. Membrane vesicles and purified F_oF_1s were analyzed by 0.1% SDS/12–20% PAGE. Proteins (≈10 μg) in membrane vesicles, and purified preparations were precipitated with trichloroacetic acid (final concentration, 2.5%), neutralized by resuspending in 1 M Tris·HCl (pH 8.8), containing 2% SDS, and subjected to electrophoresis. Proteins were visualized with Coomassie brilliant blue R or immunoblotting. Preparation of F_1-stripped membrane vesicles was carried out as follows. Membrane vesicles of *E. coli* cells were prepared by using PA6 buffer (10 mM Hepes·KOH/10% glycerol) instead of PA3-buffer (10 mM Hepes·KOH/5 mM $MgCl_2$/10% glycerol). The vesicles (500 μl) were diluted 5-fold with 2 mM EDTA and incubated at 35°C for 20 min. The membrane vesicles were collected by centrifugation at 244 $k \times g$ for 20 min, resuspended in 3 ml of 0.5 mM EDTA containing 1 mM DTT, and incubated at 35°C for 20 min. The membrane vesicles were again collected by centrifugation (244 $k \times g$ for 20 min) and resuspended in 300 μl of PA3.

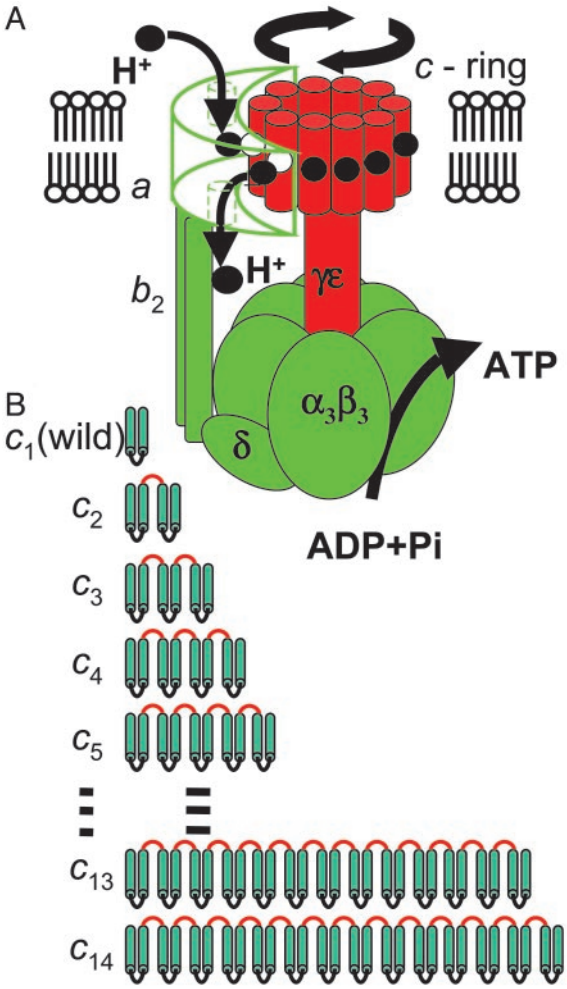

Fig. 1. Rotary model for ATP synthesis by F_oF_1 and diagram of the fused F_oc subunits (c_n) used in this study. (*A*) Proton transport through F_o drives rotation of *c*-ring made of a certain number (*n*) of F_oc subunits. According to the current model (6, 7), each proton enters the assembly through a half-channel of F_oa subunit accessible from periplasmic side and binds to the E56 carboxylate of one of the F_oc subunits that is interacting with the F_oa. The F_oc with the protonated binding site then moves from the F_oa interface region into the lipid-surrounded region in the membrane, and after $n - 1$ steps, the proton is released into another half-channel of F_oa that is open to the cytoplasmic side. One complete revolution of the *c*-ring accompanies the transport of *n* protons across membrane and produces three ATP molecules at F_1 through rotation of γ-ε subunits that are connected to *c*-ring. (*B*) Genetically fused F_oc multimers used in this study. The wild-type F_oc, called c_1 in this article, is a hairpin-structured membrane protein consisting of 72 aa. We made 13 mutant F_oF_1s with c_2–c_{14}. Linker portions are shown in red.

Analytical Procedures. F_1 of thermophilic *Bacillus* PS3 was purified by using the procedures described in ref. 17. ATPase activity was measured with an ATP-regenerating system at 45°C in 50 mM Hepes·KOH buffer (pH 7.5), containing 100 mM KCl, 5 mM $MgCl_2$, 1 mM ATP, 1 μg/ml *p*-trifluoromethoxyphenylydrazone (FCCP), 2.5 mM KCN, 2.5 mM phosphoenolpyruvate, 100 μg/ml pyruvate kinase, 100 μg/ml lactate dehydrogenase, and 0.2 mM NADH (17). Hydrolysis of 1 μmol of ATP per min is defined as one unit. The slopes of decreasing absorbance at 340 nm in the steady-state phase (400–600 sec) were used for the calculation of the activity. Sensitivity of the ATP hydrolysis activity to inactivation by *N*,*N*′-dicyclohexylcarbodiimide (DCCD) was analyzed by the same method as used in the previous study (13). ATP-driven H^+-pumping activity was measured as quenching of the fluorescence (excitation, 410 nm; emission, 480 nm) of 9-amino-6-chloro-2-methoxyacridine (ACMA) in 10 mM Hepes·KOH, pH 7.5/100 mM KCl/5 mM $MgCl_2$, supplemented with membrane vesicles (0.5 mg of protein per ml) and ACMA (0.3 μg/ml) at 45°C (17). The reaction was initiated by adding 1 mM ATP, and quenching reached a steady level after 1 min. After 5 min, FCCP (1 μg/ml) was added and reversal of fluorescence was confirmed. The magnitude of fluorescence quenching at 3 min relative to the level after addition of FCCP was taken as the proton-pumping activity. Activity of c_n-F_o (n = 9–12) as a proton channel was measured for the F_1-stripped membrane vesicles with attenuation of NADH-induced ACMA fluorescence quenching. The solution contained F_1-stripped membrane vesicles (0.1 mg of membrane protein per ml) and ACMA (0.3 μg/ml) in 10 mM Hepes·KOH, pH 7.5/100 mM KCl/5 mM $MgCl_2$ with or without 50 μM purified F_1. The electrochemical potential of protons was generated by adding 0.3 mM NADH, and the effect of the addition of F_1 on the magnitude of fluorescence quenching was monitored. The reaction was terminated by adding 1 μg/ml of FCCP. ATP synthesis activity was measured (18) as follows. The solution (200 μl) containing 30 mM Hepes·KOH, pH 7.5/50 mM KCl/5 mM $MgCl_2$/5 mM ADP/25 mM KPi/5% glycerol were mixed with 50 μl of membrane vesicles (50 μg of protein) and incubated at 45°C for 5 min. The reaction was initiated by supplementing 2 mM NADH. After 0, 2, 6, 10, and 20 min, aliquots of the reaction mixture were transferred to another tube and mixed with trichloroacetic acid to a final concentration of 2.5% to terminate the reaction. The pH was adjusted to 7.7 by adding 125 mM Tris·acetate (pH 9.5), and the amount of ATP was determined with the CLSII ATP bioluminescence assay kit (Roche). It was confirmed that ATP synthesis did not occur when FCCP was present. Protein concentrations were determined by using the BCA protein assay kit (Pierce), with BSA as a standard.

Free-Energy Functions Used in the Elastic γ Rotation Model. $V_{Fo}(\theta_{Fo})$ and $V_{F1}(\theta_{F1})$ are expressed by smooth cosine functions with minima at every 36° rotational step for F_o, as revealed in the present study, and every 40° and 80° rotational substeps for F_1,

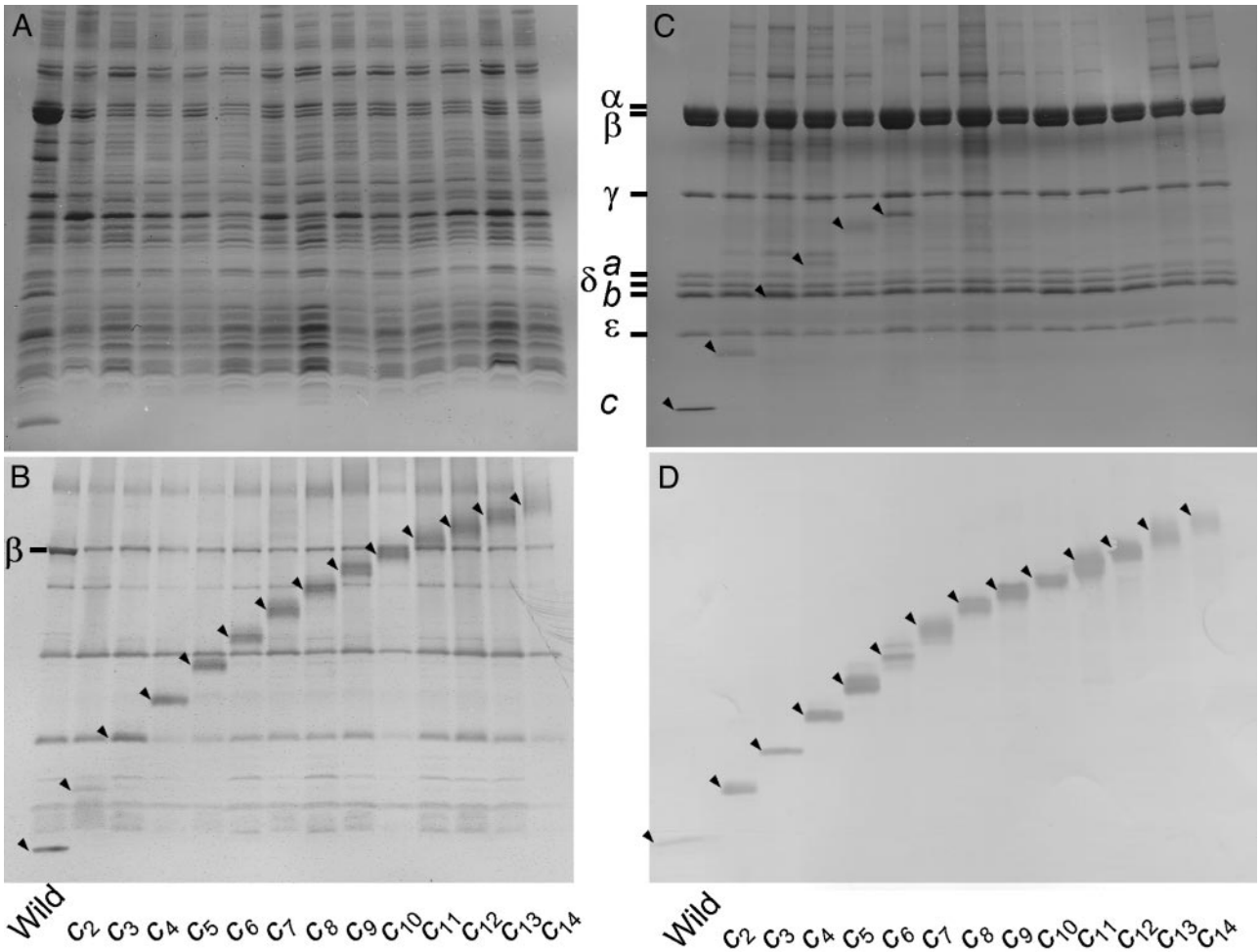

Fig. 2. Expression and purification of c_n-F_oF_1s. Proteins were analyzed with SDS/PAGE and visualized with Coomassie brilliant blue (*A* and *C*) or with immunoblotting by using anti-F_oc antibodies (*B* and *D*). Bands of c_n were hardly stained with usual protein staining methods and were shown with immunoblotting. (*A* and *B*) Membrane vesicles prepared from *E. coli* cells expressing c_n-F_oF_1s (n = 1–14). For reference, the bands of β subunit of F_1 were also visualized with anti-β antibodies (*B*). (*C* and *D*) Purified c_n-F_oF_1s. The positions of c_n are indicated by arrowheads.

corresponding to the substeps of the γ rotation in F_1 observed by single-molecule observations (19–21), respectively. The energy-barrier heights separating the minima in $V_{Fo}(\theta_{Fo})$ and $V_{F1}(\theta_{F1})$, which also relates to the widths of the free-energy basins, are assumed to be 4 kcal/mol to mimic discrete stepping motions of the γ rotation observed in single-molecule experiments (19–21). It was confirmed that the essential features of the γ rotation reported here hold in a wide range of the barrier-height parameters (1–8 kcal/mol) through constructing several free-energy surfaces by changing values of the parameters. Overall, decrease by 32 kcal/mol and increase by 24 kcal/mol per revolution are then included in $V_{Fo}(\theta_{Fo})$ and $V_{F1}(\theta_{F1})$ to represent the proton gradient across membrane at F_o and costs of three ATP productions at F_1, respectively. The elastic energy of the γ torsion is taken into account by a harmonic function, $1/2k(\theta_{Fo}-\theta_{F1})^2$, with a force constant k of 0.01 k_bT, which gives rise to $\approx$10° thermal fluctuation of the free γ-subunit torsion.

Results

Expression and Purification of c_n-F_oF_1s. To determine the copy number in the functional complex, we made a series of 13 kinds of thermophilic F_oF_1s that had multimer c_n (n = 2–14) in which C termini of F_oc subunits were fused genetically to N termini of adjacent F_oc subunits with a linker sequence, Gly-Ser-Ala-Gly (Fig. 1*B*) and measured their functional activities. These c_n-F_oF_1s were expressed in the membranes of the host *E. coli* cells. Membrane vesicles were prepared from the cells and analyzed with SDS/PAGE. Protein bands of the α and β subunits were seen in protein staining (Fig. 2*A*), and protein bands of c_n were visualized by immunoblotting (Fig. 2*B*). Estimated from band intensities in immunoblotting with anti-β antibody, the amounts of expressed mutant F_oF_1s in the membranes were 20–30% of the wild-type c_1-F_oF_1 (Fig. 2*B*). Apparent proteolytic degradation was not observed for c_n. The c_n-F_oF_1s were solubilized individually from the membranes and isolated by nickel–nitrilotriacetic acid (Ni-NTA) affinity chromatography. Free c_n uncomplexed with other subunits, if it exists, was removed by His tags attached to the β subunits. The isolated c_n-F_oF_1s showed clearly the bands of all subunits of the F_oF_1s except for the bands of c_n that were poorly stained with Coomassie blue (Fig. 2*C*). Immunoblotting with anti-F_oc antibody, however, clearly indicated the presence of c_n at the expected positions (Fig. 2*D*). Judging from relative intensities of the bands, it appears that all of the c_n-F_oF_1s can assemble normally despite the alterations in the c subunits.

Functions of c_n-F_oF_1s in the Membrane Vesicles. ATP hydrolysis activities derived from the expressed c_n-F_oF_1s in the membrane vesicles were compared (Fig. 3*A*). To assess the amount of functional F_oF_1, we measured ATP hydrolysis activity with or

BIOCHEMISTRY

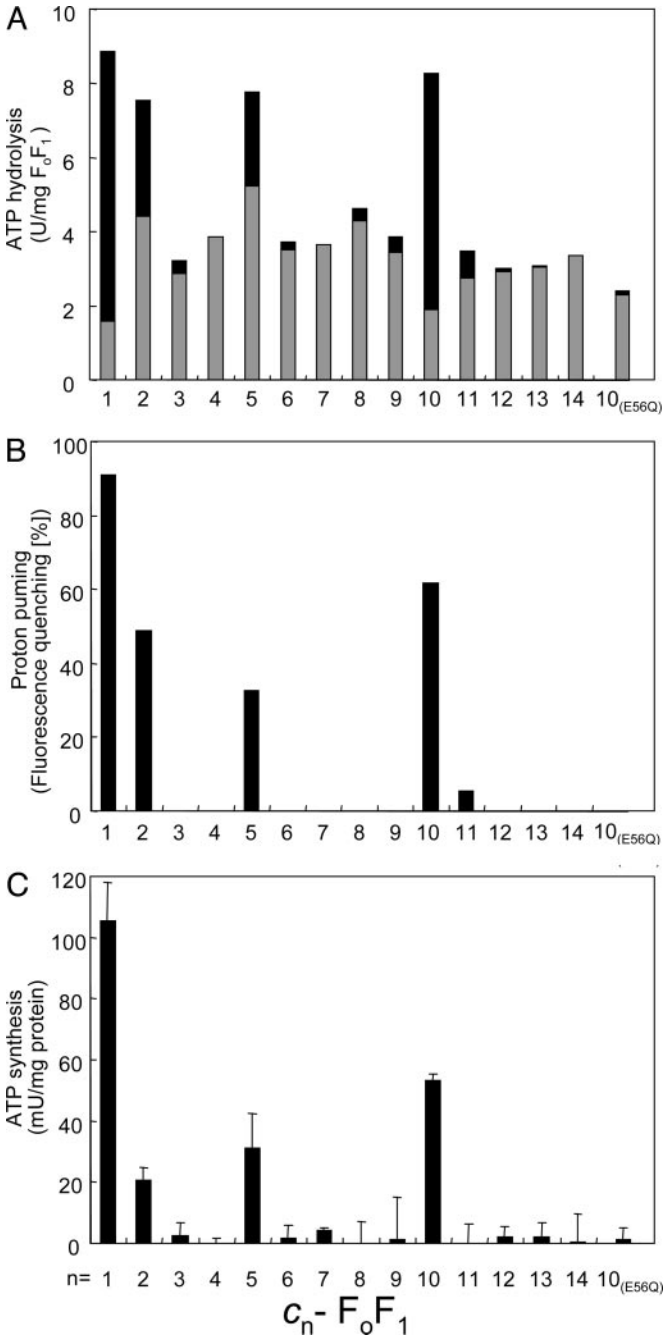

Fig. 3. ATP hydrolysis, proton pumping, and ATP synthesis activities of membrane vesicles containing c_n-F_oF_1s. The rightmost bars [$c_{10(E56Q)}$] show the results of $c_{10(E56Q)}$-F_oF_1. (*A*) ATP hydrolysis activities of the membrane vesicles that contained c_n-F_oF_1. Black and gray portions of the bars represent the DCCD-sensitive and -resistant fractions of activities, respectively. (*B*) ATP-driven proton-pumping activities measured with ACMA fluorescence quenching. The relative magnitude of quenching induced by addition of ATP is shown. (*C*) ATP synthesis driven by NADH oxidation. The amounts of synthesized ATP after addition of NADH were measured, and the rates of ATP increase are shown. Experimental details are described in *Materials and Methods*.

without pretreatment by DCCD. This reagent is known to label specifically a critical glutamic acid residue in F_oc, and it blocks proton translocation and rotation of the *c*-ring (and hence, γ-ε of F_1). With rotation being prevented by DCCD, ATP hydrolysis (and ATP synthesis) cannot occur in the coupled F_oF_1 complex. However, when the connection between F_1 and F_o is defective, the F_1 component can hydrolyze ATP uncoupled to H^+ translocation. Therefore, the DCCD-sensitive fraction of ATP hydrolysis activity corresponds to the functional F_oF_1 in which the proton translocation, ATP hydrolysis, and ATP synthesis are properly coupled by rotation of the central rotor. For the wild-type c_1-F_oF_1, 85% of the ATP hydrolysis activity was DCCD-sensitive (Fig. 3*A*, black bars) and 15% was resistant (Fig. 3*A*, gray bars). Among c_n-F_oF_1s, only c_2-, c_5-, and c_{10}-F_oF_1s showed significant DCCD-sensitive ATP hydrolysis activities, with c_{10}-F_oF_1 being the highest. ATP hydrolysis activities of other c_n-F_oF_1s were low (less than half of the wild-type c_1-F_oF_1) and not affected by DCCD.

Next, the proton-pumping driven by ATP hydrolysis was tested with the membrane vesicles containing c_n-F_oF_1s (Fig. 3*B*). Proton-pumping into vesicles was monitored as acidification of the lumen of the vesicles by fluorescence quenching of ACMA, and the degree of induced quenching was taken as the proton-pumping activity. As shown, only c_2-, c_5-, and c_{10}-F_oF_1s, as well as the wild-type c_1-F_oF_1, showed the proton-pumping activities in response to the addition of ATP. Purified c_{10}-F_oF_1 reconstituted into liposomes also exhibited the same ATP-driven proton-pumping activity (data not shown). We also monitored protons pumped into the membrane vesicles by oxidation of NADH through the respiratory chain. Upon addition of NADH, instead of ATP, to the vesicles, similar ACMA quenching was observed for all membrane vesicles containing c_n-F_oF_1s (data not shown), indicating that the protons pumped into the membrane vesicles were retained in the lumens of the vesicles and any c_n-F_oF_1s did not increase proton leakage of the membranes. When NADH, ADP, and phosphate were given, membrane vesicles containing c_2-, c_5-, and c_{10}-F_oF_1s exhibited the synthesis of ATP with 18%, 27%, and 50% yields, respectively, compared with the wild-type c_1-F_oF_1 (Fig. 3*C*). Other c_n-F_oF_1s did not exhibit ATP synthesis activity. In summary, even though all of c_n-F_oF_1s can form stable F_oF_1 complexes, the capacity to couple proton transport to ATP synthesis and hydrolysis is observed only with c_{10}-F_oF_1 and, to a lesser extent, c_2- and c_5-F_oF_1s. The activities of c_2- and c_5-F_oF_1s are explained by assuming that five copies of c_2 and two copies of c_5 can substitute, although inefficiently, the role of 10 copies of F_oc in the wild-type c_1-F_oF_1. The generation of the functional c_{10}-F_oF_1 allows one to carry out experiments that are otherwise difficult. For example, when only a single E56Q mutation was introduced into the first hairpin unit of the c_{10}, the resulting membrane vesicles containing c_{10}-F_oF_1 did not catalyze ATP-driven proton pumping or ATP synthesis (Fig. 3). Therefore, the E56Q substitution in a single copy of the naturally occurring *c*-ring is sufficient to abolish H^+ translocation coupled to ATP synthesis and hydrolysis. This result provides evidence that each of all 10 E56 in the *c*-ring is indispensable. Studies have suggested a similar conclusion (22, 23), but they were based on statistical introduction of the mutation or DCCD-labeling into the *c*-ring.

Proton-Channel Activities of c_9-, c_{10}-, c_{11}-, and c_{12}-F_o. Another intriguing question is whether c_n fusion proteins that are incapable of participating in proton translocation during ATP synthesis and hydrolysis are capable of participating in passive proton diffusion. EDTA treatment of the membrane vesicles removed F_1 portions from ≈90% of c_n-F_oF_1s, leaving F_1-stripped c_n-F_o vesicles. NADH was used to generate a proton gradient across membranes that was monitored with fluorescence quenching of ACMA. If F_o acts as a proton channel and mediates passive proton diffusion, the proton gradient is dissipated and fluorescence quenching should be attenuated. The inclusion of F_1 should increase the quenching because it binds to F_o to block the channel. We tested membrane vesicles containing c_9-, c_{10}-, c_{11}-, and c_{12}-F_os as well as the wild-type c_1-F_o (Fig. 4). For c_1-F_o, the quenching was very small in the absence of F_1 but large in the

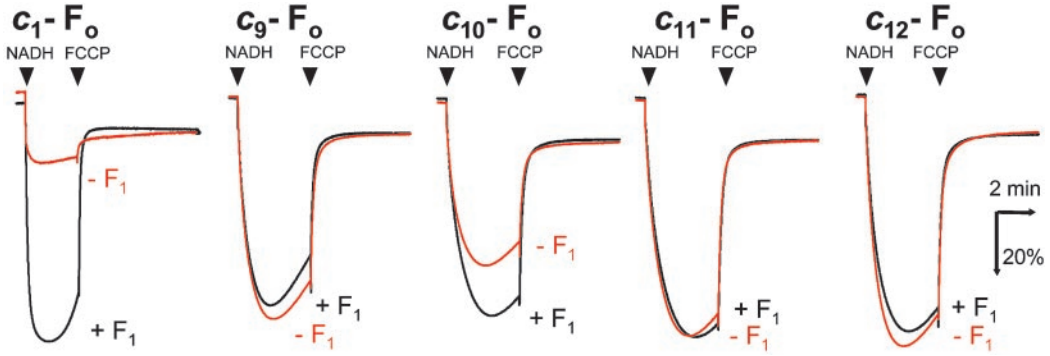

Fig. 4. Activities of c_9-, c_{10}-, c_{11}-, and c_{12}-F_os as a proton channel. The activity of F_o as a proton channel was assessed from the ACMA fluorescence quenching in the presence (black traces) or absence (red traces) of F_1. Proton leak was detected as attenuation of the quenching and restoration of the quenching by F_1 ensured the specific leak through F_o. The reactions were started by addition of NADH and terminated by addition of FCCP. The results for the wild-type c_1-F_o are shown as a reference. Experimental details are described in *Materials and Methods*.

presence of F_1. Among c_9-, c_{10}-, c_{11}-, and c_{12}-F_os, only c_{10}-F_o showed the attenuated quenching in the absence of F_1 and the increased quenching by the inclusion of F_1. Others did not show such characteristic quenching behavior but showed simple quenching in both the presence and absence of F_1, implying a loss of the proton channel activity. The degree of attenuation of c_{10}-F_o vesicles was less than that of c_1-F_o vesicles, and it was partly due to the relatively low content of c_{10}-F_o in the membranes. Thus, the proton transport through F_o requires very strict arrangement of contact surface between F_oa and F_oc in the F_o assembly and even a rotary displacement as tiny as 3.3° (360°/10–360°/11) seems to be enough to disable a proton transfer between them.

Discussion

From the results described here, we conclude that the naturally occurring F_oF_1 of the thermophilic *Baccilus* PS3 contains 10 copies of F_oc subunits in the *c*-ring. In the case of *E. coli* F_oF_1, even though the preferred copy number of F_oc in the *c*-rings is believed to be 10, it has been argued that a *c*-ring composed of eight or nine F_oc subunits can have at least partial function (12) and that the copy number of F_oc can vary depending on the growth conditions (24). However, our results show that such ambiguity of the copy number of F_oc would not be allowed, and the *c*-ring of the functional *E. coli* F_oF_1 is most likely constituted by 10 copies of F_oc under any conditions. Another possibility is that the greater flexibility of the longer linker sequence (10 or 13 aa) in *E. coli* fused F_oc (12) may allow a *c*-ring of nine subunits ($3 \times c_3$) to function even though the packing is not perfect as in an optimal *c*-ring of 10 subunits.

Given that the *c*-ring of our F_oF_1 is made of 10 F_oc subunits, step sizes of unit-rotation do not fit between F_1 and F_o. If the *c*-ring were a dodecamer, the unit-rotation angle by a single proton transport is 30° and four unit-rotations give rise to a 120° rotation of the γ-subunit that produces one ATP at F_1. The unit-rotation angle of the decamer *c*-ring, however, must be 36°, and a 120° rotation of the γ-subunit cannot be a multiple of a 36° rotation. During rotation, the catalytic events at F_1 may occur only at the moments when γ–β interfaces are aligned precisely to give the most suitable geometries of catalytic sites. These moments are realized by experiments as dwelling times of F_1 rotation, and at least two kinds of them have been identified to date in a 120° rotation, ATP-waiting dwell (0°) and catalytic dwell (80°) (19–21). Therefore, rotation with a 36° unit at F_o must be adjusted to these dwelling positions at F_1 by some means. Slip at the connection between γ–ε and the *c*-ring does not occur during rotation because a cross-linking between them does not impair the activities of F_oF_1 (3). Because the coiled-coil structure

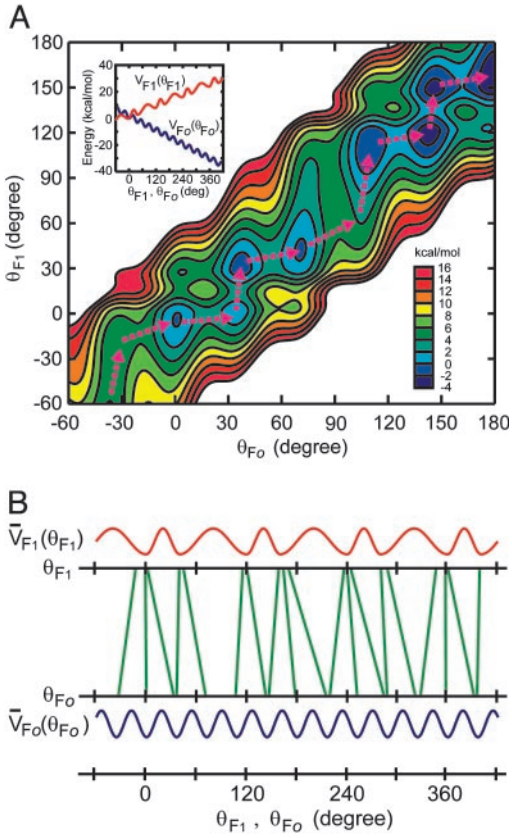

Fig. 5. Model of the rotation of an elastic γ in the ATP-synthetic process of c_{10}-F_oF_1. (*A*) Contour plot of the modeled free-energy surface of the γ rotation in c_{10}-F_oF_1 in terms of rotational angles of γ at the F_o and F_1 interfaces, which are θ_{Fo} and θ_{F1}, respectively. The free-energy surface possesses several minima, and the rotational motion of γ is regarded as transitions between the minima. Pink dashed arrows indicate energetically preferable paths of the transitions for the ATP synthetic process, indicating temporal gaps between the rotations of θ_{Fo} and θ_{F1}. The free-energy surface was constructed with free-energy functions $V_{Fo}(\theta_{Fo})$ and $V_{F1}(\theta_{F1})$ (*Inset*), representing inherent free-energy profiles along the rotations at the F_o and F_1 interfaces, respectively, and a harmonic term of the elastic γ torsion connecting the rotations of those interfaces. Detailed functional forms of those energy components are described in *Materials and Methods*. (*B*) Twisting of γ in the course of the γ rotation. Green lines connect values of θ_{Fo} and θ_{F1} at the minima of the free-energy surface in the γ rotation shown in *A*. Tilt of the green lines from the vertical, therefore, indicates the twisting of γ. Note that the θ_{Fo} and θ_{F1} values are within narrow range around the energy minima of $\bar{V}_{Fo}(\theta_{Fo})$ and $\bar{V}_{F1}(\theta_{F1})$, representing the oscillatory energy parts along θ_{Fo} and θ_{F1}, respectively.

BIOCHEMISTRY

of the γ subunit allows some internal twisting and the $F_o b_2$ subunits of the side stalk have extra flexibility (25), they can undergo elastic twisting or bending (26, 27) to enable the proper alignment of rotor–stator contacts at both F_o and F_1. Assuming that the γ subunit takes this task with its torsional spring constant being in the range allowing $\approx 10°$ thermal fluctuation, we calculated how it rotates with twisting itself (Fig. 5). The model shows that the rotations of γ at the F_o and F_1 interfaces do not coincide with each other but evolve with temporal gaps between them permitted by the elasticity of γ (Fig. 5*A*). The twisting angle of γ at the energy minima in the course of the γ rotation is mainly distributed in the range of 0–30°, but it reaches to $\approx 40°$ at the maximum (Fig. 5*B*). The flexibility of γ allows both the F_o-γ and F_1-γ interfaces at the free-energy minima to stay in conformations adequate for the proton transport in F_o and the catalysis in F_1 despite the step-size mismatch, providing sufficient time for those events to take place.

Another important consequence of the decamer *c*-ring is that 10 protons are required for the synthesis of three ATPs. This noninteger H^+/ATP (10:3) ratio means that one molecule of ATP is produced by transport of three protons on one occasion but four protons on another occasion. Therefore, microscopic couplings between events at F_o and those at F_1 cannot be strict like a meshed gear but rather "permissive;" consecutive transports of three protons at F_o, for example, do not necessarily require to accompany three corresponding elementary catalytic steps of ATP synthesis at F_1. It is easily understood that the microscopic coupling should be permissive if the central rotor-shaft twists during rotation, as described in the previous paragraph. Here, we report the permissive nature of the coupling between proton transport and ATP synthesis of F_oF_1, but such nature of the coupling can be general among other biological motor systems to connect critical well tuned microscopic events in the large domain motions.

Finally, we have made a functional F_oF_1 that has a single polypeptide *c*-ring of genetically fused decamer of F_oc. A recent genome project of an achaebacterium, *Methanopyrus kandleri* has revealed the presence of a single gene for *c*-ring consisting of 13 repeats of the hairpin domains (28). Thus, nature has already made a single-polypeptide version of the *c*-ring.

We thank J. Suzuki for F_1 preparation and R. Iino, T. Masaike, H. Imamura, T. Ariga, H. Ueno, K. Shimabukuro, T. Hisabori, E. Muneyuki, M. Motojima, and N. Sone for helpful discussions. N.M. is supported by research fellowships from the Japan Society for the Promotion of Science for Young Scientists.

1. Boyer, P. D. (1997) *Annu. Rev. Biochem.* **66,** 717–749.
2. Yoshida, M., Muneyuki, E. & Hisabori, T. (2001) *Nat. Rev. Mol. Cell Biol.* **2,** 669–677.
3. Tsunoda, S. P., Aggeler, R., Yoshida, M. & Capaldi, R. A. (2001) *Proc. Natl. Acad. Sci. USA* **98,** 898–902.
4. Noji, H., Yasuda, R., Yoshida, M. & Kinosita, K. J. (1997) *Nature* **386,** 299–302.
5. Yasuda, R., Noji, H., Kinosita, K. J. & Yoshida, M. (1998) *Cell* **93,** 1117–1124.
6. Junge, W., Lill, H. & Engelbrecht, S. (1997) *Trends. Biochem. Sci.* **22,** 420–423.
7. Vik, S. B., Patterson, A. R. & Antonio, B. J. (1998) *J. Biol. Chem.* **273,** 16229–16234.
8. Stock, D., Leslie, A. G. & Walker, J. E. (1999) *Science* **286,** 1700–1705.
9. Stahlberg, H., Muller, D. J., Suda, K., Fotiadis, D., Engel, A., Meier, T., Matthey, U. & Dimroth, P. (2001) *EMBO Rep.* **2,** 229–233.
10. Seelert, H., Poetsch, A., Dencher, N. A., Engel, A., Stahlberg, H. & Muller, D. J. (2000) *Nature* **405,** 418–419.
11. Seelert, H., Dencher, N. A. & Muller, D. J. (2003) *J. Mol. Biol.* **333,** 337–344.
12. Jiang, W., Hermolin, J. & Fillingame, R. H. (2001) *Proc. Natl. Acad. Sci. USA* **98,** 4966–4971.
13. Suzuki, T., Ueno, H., Mitome, N., Suzuki, J. & Yoshida, M. (2002) *J. Biol. Chem.* **28,** 13281–13285.
14. Landt, O., Grunert, H. P. & Hahn, U. (1990) *Gene* **96,** 125–128.
15. Kunkel, T. A., Roberts, J. D. & Zakour, R. A. (1987) *Methods Enzymol.* **154,** 367–382.
16. Jones, P. C. & Fillingame, R. H. (1998) *J. Biol. Chem.* **273,** 29701–29705.
17. Suzuki, T., Suzuki, J., Mitome, N., Ueno, H. & Yoshida, M. (2000) *J. Biol. Chem.* **275,** 37902–37906.
18. Schulenberg, B. & Capaldi, R. A. (1999) *J. Biol. Chem.* **274,** 28351–28355.
19. Yasuda, R., Noji, H., Yoshida, M., Kinosita, K. J. & Itoh, H. (2001) *Nature* **410,** 898–904.
20. Shimabukuro, K., Yasuda, R., Muneyuki, E., Hara, K. Y., Kinosita, K. J. & Yoshida, M. (2003) *Proc. Natl. Acad. Sci. USA* **100,** 14731–14736.
21. Nishizaka, T., Oiwa, K., Noji, H., Kimura, S., Muneyuki, E., Yoshida, M. & Kinosita, K. J. (2004) *Nat. Struct. Mol. Biol.* **11,** 142–148.
22. Hermolin, J. & Fillingame, R. H. (1989) *J. Biol. Chem.* **264,** 3896–3903.
23. Dmitriev, O. Y., Altendorf, K. & Fillingame, R. H. (1995) *Eur. J. Biochem.* **233,** 478–483.
24. Schemidt, R. A., Qu, J., Williams, J. R. & Brusilow, W. S. (1998) *J. Bacteriol.* **180,** 3205–3208.
25. Sorgen, P. L., Bubb, M. R. & Cain, B. D. (1999) *J. Biol. Chem.* **274,** 36261–36266.
26. Oster, G. & Wang, H. (2000) *Biochim. Biophys. Acta* **1458,** 482–510.
27. Junge, W., Panke, O., Cherepanov, D. A., Gumbiowski, K., Muller, M. & Engelbrecht, S. (2001) *FEBS Lett.* **504,** 152–160.
28. Lolkema, J. S. & Boekema, E. J. (2003) *FEBS Lett.* **543,** 47–50.